# Development of a PM<sub>2.5</sub> sampler with inertial impaction for sampling airborne particulate matter

Panich Intra\*, Artit Yawootti\*, Usanee Vinitketkumnuen\*\*, and Nakorn Tippayawong\*\*\*

\*College of Integrated Science and Technology, Rajamangala University of Technology Lanna, Chiang Mai, 50300, Thailand 
\*\*Department of Biochemistry, Faculty of Medicine, Chiang Mai University, Chiang Mai, 50200, Thailand 
\*\*\*Department of Mechanical Engineering, Faculty of Engineering, Chiang Mai University, Chiang Mai, 50200, Thailand 
(Received 23 December 2010 • accepted 15 December 2011)

**Abstract-**A simple and low cost  $PM_{2.5}$  impactor for sampling airborne particulate matter was developed, designed and evaluated. The design was an assembly of an acceleration nozzle and an impaction plate. Particles with sufficient inertia were unable to follow air streamlines and impacted on the plate. Smaller particles followed the streamlines, avoided being captured by the plate and could then be collected on a downstream filter. Analytical and numerical models were formulated to predict collection efficiency, flow fields and vectors, and particle trajectories in the impactor. The modeling suggested that an optimal operational domain exists for the  $PM_{2.5}$  impactor. A prototype was then built and tested. The collected particles on the impaction plate and downstream of the  $PM_{2.5}$  impactor were analyzed by using scanning electron microscopy. Experimental results agreed well with the theoretical predictions. Testing of the  $PM_{2.5}$  impactor prototype showed promising results for this airborne particulate matter sampler.

Key words: Particulate Matter, PM<sub>2.5</sub>, Impactor, Numerical Model, SEM

#### INTRODUCTION

A recent particulate air pollution episode adversely affected Chiang Mai, Thailand. In 2008 extensive burning of forests [1] to make room for agricultural land created conditions that were hazardous to health. Therefore, the study of aerosols accelerated. Any solid or liquid material suspended in air with aerodynamic diameter in the range of 1 nm to 100 µm can be considered as particulate matter (PM). Since the U.S. Environmental Protection Agency (EPA) promulgated a new regulation for the mass concentration of suspended aerosol particles with aerodynamic diameter lower than 2.5 µm, which are referred to as PM<sub>2.5</sub>, the investigation of fine particles has focused on the measuring and monitoring of this aerosol fraction [2]. PM<sub>25</sub> can penetrate the alveoli and bypass the upper respiratory tract because they are small enough to allow deposition at places where they can do the most damage. The hazard caused by PM25 depends on the chemical composition of PM<sub>2.5</sub> and on the site where they are deposited within the human respiratory system [3].

Sampling and measurement of the concentration of PM<sub>2.5</sub> in the ambient atmosphere is an important step in atmospheric aerosol determination in order to evaluate the degree of hazard it poses. A PM<sub>2.5</sub> sampler is one of the valuable tools for these applications. Many PM<sub>2.5</sub> samplers have been developed for separating airborne aerosol particles for further chemical composition analysis. These instruments are mostly based on a modified impactor [4], a virtual impactor [5], or a cyclone [6]. A widely used sampler is the inertial impactor because of its simple operation and high separation and collection capabilities [7]. It consists of an acceleration nozzle and a flat plate, called an impaction plate. In this instrument particles

with sufficient inertia are unable to follow air streamlines and will impact on the impaction plate. Smaller particles follow the streamlines, avoid being captured by the plate and can then be collected on a downstream filter. The aerodynamic particle size at which the particles are separated is called the cut-point diameter. There are numerous studies on the development and investigation of the inertial impactor for mass concentration and size distribution measurements of nanoparticles, PM<sub>2.5</sub> and PM<sub>10</sub> [8-25]. Inertial impactors also have been used to remove submicron-sized particles that are outside the measurement size range upstream of the electrical mobility spectrometer because of their contribution to multiple-charged aerosols [7]. The effects of impactor design and flow conditions on the determination of aerosol size distribution have been studied analytically. Several primary studies described the underlying principles governing impactor design [8-10,12,22,23]. Subsequent studies focused on improving and characterizing the performance of impactors, as well as developing impactors for specific applications [13-

There have been only a few scanning electron microscopy (SEM) observations on any configuration of the PM<sub>2.5</sub> impactor--information that would be very useful in the design of an impactor. Knowledge of the nature of the particles collected on the impactor plate may be important to the solution of problems [9] commonly occurring in impactor operation like particle bounce and entrainment. In addition, a well-designed impactor should be easy and inexpensive to manufacture, simple to operate, require no moving parts during sampling provide easy maintenance, require no attendance over multiple days, and provide sustained operation at high loadings [3]. Theoretical models could be used to analyze the collection efficiency, fluid flow field and vector, and particle trajectory in the impactor. This information could then be used to build a prototype, evaluate it experimentally, and give information of cost and ease of opera-

<sup>&</sup>lt;sup>†</sup>To whom correspondence should be addressed. E-mail: panich\_intra@yahoo.com

tion. These are the goals of this study. SEM analysis was also used to observe the collected particles on the impaction plate and downstream of the PM<sub>25</sub> impactor.

# DESIGN OF THE PM<sub>25</sub> IMPACTOR

The PM<sub>2.5</sub> impactor was designed to sample airborne particulate matter with sizes smaller than 2.5 µm based on their aerodynamic diameter. The primary performance requirements of the PM<sub>2.5</sub> impactor are dictated by inertia and expressed in the collection efficiency of the aerosol. The most important characteristic of an inertial impactor is the associated collection efficiency curve, which indicates percentage of particles of any size collected on the plate as a function of the particle diameter [8-12]. Key parameters are the curve sharpness and the cut point diameter (i.e., the aerodynamic diameter which corresponds to an efficiency of 50%), which in our case should be 2.5 µm. According to Marple and Willeke [9], the aerosol flow rate, the acceleration nozzle-to-impaction plate distance, and the acceleration nozzle diameter are the important parameters goveming the performance of the inertial impactor. The nozzle diameter can be calculated from the Stokes number (Stk). The Stokes number is a dimensionless parameter that characterizes impaction, defined as the ratio of the particle stopping distance to the half-width or the radius of the impactor throat. The Stokes number equation for a round jet impactor is defined as [9]:

$$Stk(\mathbf{d}_p) = \frac{4\rho_p C_c \mathbf{d}_p^2 Q}{9\pi n \mathbf{D}^3}.$$
 (1)

where  $\rho_p$  is the particle density,  $C_e$  is the Cunningham slip correction factor,  $d_p$  is the particle diameter, Q is the aerosol flow rate,  $\eta$  is the gas viscosity, and D is the acceleration nozzle diameter. Thus, the particle cut-off diameter at 50% collection efficiency,  $d_{50}$ , can be calculated by [9]

$$d_{50} = \sqrt{\frac{9\pi\eta D^{3} Stk_{50}(d_{50})}{4\rho_{0}C_{c}Q}}$$
 (2)

The particle collection efficiency of the impactor is determined from [15]

$$n(d_n) = [1 + (d_{50}/d_n)^{2s}]^{-1}$$
(3)

where s is the parameter affecting the steepness of the collection efficiency curve. For an ideal impactor without wall losses, s=1 is arbitrarily assumed for the steepness of the collection efficiency curve [26]. Therefore, the mass concentration of aerosol particles,  $m_p(d_p)$ , as a function of a particle diameter at the outlet of the PM<sub>2.5</sub> impactor is given by

$$m_{\nu}(d_{\nu}) = m_{0}(d_{\nu}) - m_{0}(d_{\nu}) \eta(d_{\nu})$$
 (4)

where  $m_0(d_p)$  is the mass concentration of particles as a function of a particle diameter at the inlet of the PM<sub>2.5</sub> impactor.

A schematic diagram of the PM<sub>2.5</sub> impactor developed in this study is shown in Fig. 1. The design was based on the configuration of Marple and Willeke [9]. In this designed PM<sub>2.5</sub> impactor, the acceleration nozzle and the impaction plate are made of PTFE (polytetrafluoroethylene) which has good electrical and mechanical properties. The advantage of PTFE is that it is lightweight and inexpensive. Unfortunately, charge accumulation on this non-conductive surface

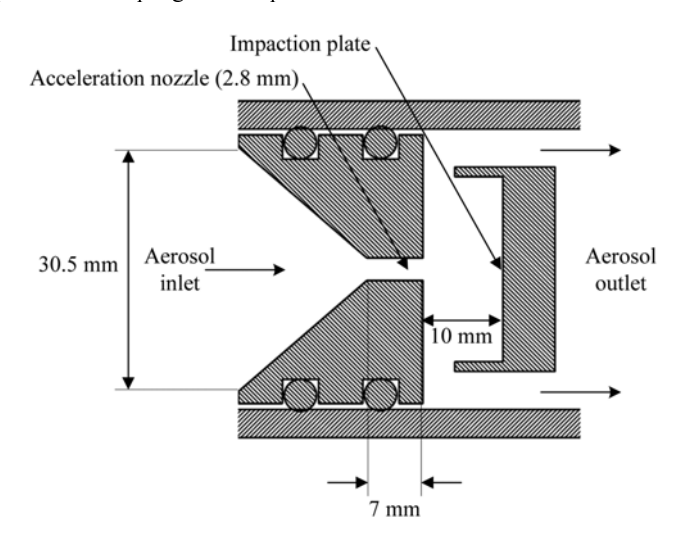


Fig. 1. Schematic diagram of the PM<sub>2.5</sub> impactor.

is likely to result in particle losses by electrostatic deposition. This loss is expected to be small because of the short exposure time. The particulate flow may be varied in the 5-15 L/min range. The acceleration nozzle diameter is 2.8 mm. The distance from the nozzle to the impaction plate is 10 mm. The impaction plate deflects the flow streamlines to a 90° bend. A numerical model was developed to investigate collection efficiency, fluid flow field and vector, and particle trajectory in the impactor. Based on the principle of momentum conservation, the continuity and the incompressible Navier-Stokes equations in 2-D cylindrical coordinates could be used in this model. For the boundary conditions, no slip boundary was applied to all the solid walls included in the computation domain. A fixed velocity boundary condition was applied to the inlet. The velocity at inlet was calculated from the flow rate through the impactor. A uniform velocity profile was assumed at the inlet across the cross section of the inlet tubes. The governing equations were numerically solved by using the commercial computational fluid dynamic software package, CFDRCTM [27]. Fig. 2 shows the computational domain and mesh used for the flow field simulations. The impactor was generated with one plane of symmetry. An unstructured grid was used. A total of about 5,282 meshes were distributed in the computational domain of the impactor.

#### **EXPERIMENTAL**

Fig. 3 shows the experimental setup used to test the performance of the  $PM_{2.5}$  impactor. The test aerosol was made by using a com-

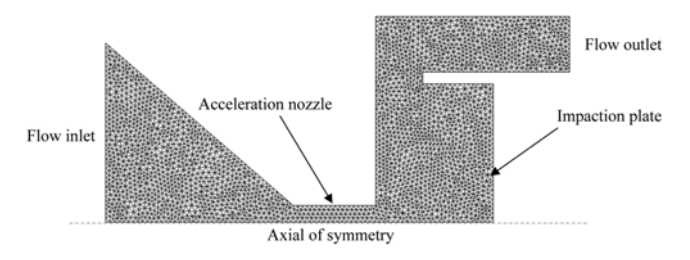


Fig. 2. Computational domain and mesh of the PM<sub>25</sub> impactor.

P. Intra et al.

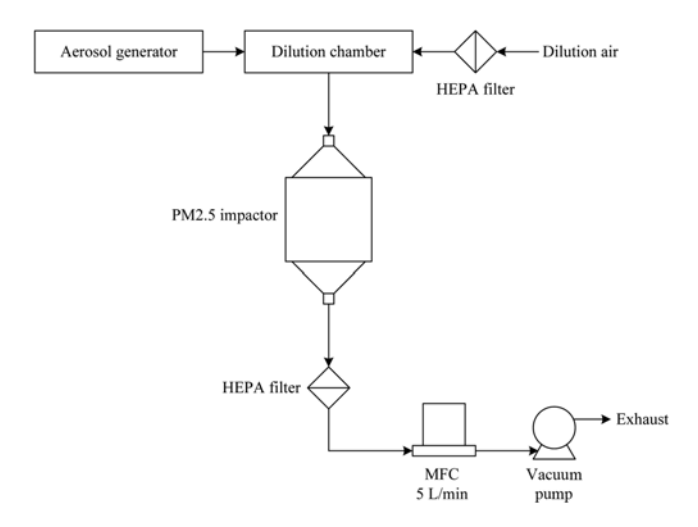


Fig. 3. Experimental setup for the performance test of the  $PM_{2.5}$  impactor.

bustion generator. A laminar diffusion burner generated the aerosol with kerosene fuel in the nominal "presooting" condition. The particle size distribution produced by the generator covered the size range from approximately 10 nm to several micrometers with particle number concentration of approximately 10<sup>14</sup> particles/m<sup>3</sup> [28]. Polydisperse aerosols were first diluted in the mixing chamber with HEPAfiltered clean air. The aerosols were then introduced to the PM2.5 impactor at a flow rate of 5 L/min. The flow rate was regulated and controlled by a mass flow meter and a controller with a vacuum pump. The particles that collected on the impaction plate of the PM<sub>2.5</sub> impactor and the filter (outlet) were later analyzed by SEM, which consisted of placing a carbon tape on the surface of the impaction plate and the filter plate to collect the aerosol. The collection lasted for at least 30 min of operation. Particle imaging was determined with a JEOL JSM-5910LV scanning electron microscope. During SEM analysis agglomerates were selected and imaged randomly to minimize bias. Magnifications between 1,500× and 30,000× were typically used, giving six to ten particles per image. By threshholding the original SEM image, the SEM projected surface area distribution was obtained first and then the projected surface area of each particle was calculated. The image was processed by using ImageJ, public domain image analysis software developed by the National Institutes of Health [29]. In the procedures, highly coagulated particles were excluded to avoid the confusion between coagulation taking place during particle growth in the gas phase or on the sampling tape during particle collection. For each data point, about 18-40 particle fields of view were used for SEM analysis. The fields, distributed throughout the sampling tape, were used to estimate particle surface area and to determine the corresponding geometric mean of the projected area diameter. This diameter, d<sub>na</sub>, can be calculated from the projected surface area, A, and is given by  $d_{pq} = \sqrt{4A/\pi}$ . To evaluate the separation performance of the PM<sub>2.5</sub> impactor at ambient condition, ambient aerosol particles were sampled with the PM<sub>2.5</sub> impactor simultaneously with currently available AIRmetrics Minivol portable air samplers at the same sampling flow rate and time. Table 1 summarizes the sampling conditions. Ambient particles were collected on glass fiber filters (Whatman, EPM2000) conditioned in a closed desiccator (room temperature of 30 degrees

Table 1. Sampling conditions

Equipments	Size range (µm)	Sampling times	Flow rate (L/min)
PM <sub>2.5</sub> impactor	PM <sub>2.5</sub>	24 hours	5
AIRmetrics minivol	$PM_{2.5}$	24 hours	5
portable sampler			

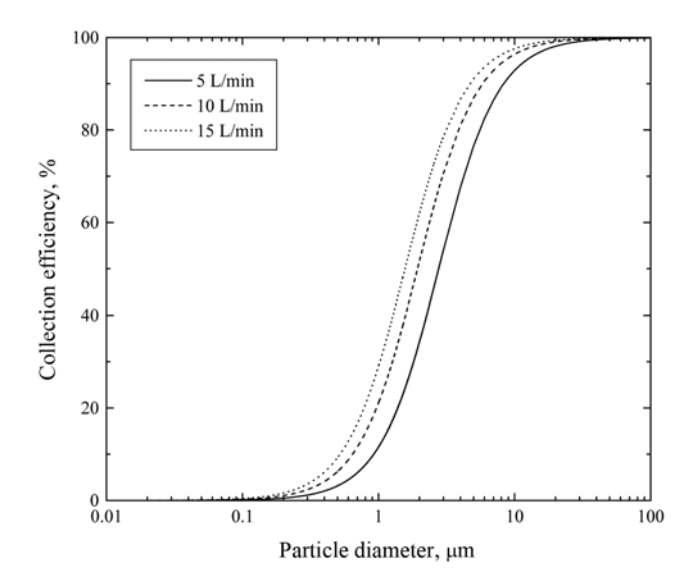


Fig. 4. Variation of theoretical collection efficiency with particle diameter at different operating flow rates.

and  $\sim$ 50% RH) for 24 hours before and after the sampling. For each set of instrument, mass collection was repeated at least three times; average values were then reported and compared.

## RESULTS AND DISCUSSION

The flow field and particle trajectory were calculated. The following values were used in the calculation: air density of 1.225 kg/ m<sup>3</sup>, viscosity of 1.7894×10<sup>-5</sup> kg/m/s, temperature of 294 K. Based on Eqs. (1)-(3), Fig. 4 shows the variation of the theoretical collection efficiency curves as a function of particle size at aerosol flow rates of 5, 10 and 15 L/min with the acceleration nozzle diameter of 2.8 mm. The calculations were done for a particle size range from 10 nm to 100 µm, and they show that the cut-off diameter decreased as the flow rate increased. For the performance of the impactor, flow rates of 5 and 15 L/min gave cut-off diameters of about 2.5 and 1.5 μm, respectively. As expected, the collection efficiency increased with flow rate because of the higher inertial force acting on the particles at higher velocities. Fig. 5 shows the theoretical prediction of particulate size distributions downstream of the PM<sub>2.5</sub> impactor, calculated, as a function of different aerosol flow rates (5, 10, and 15 L/ min), for an upstream size distribution that is typical of ambient conditions [30]. A significant portion of the aerosol mass at the inlet (about 80%) was removed by the impactor.

Fig. 6 gives the flow pattern in the impactor as velocity field and vector plots as well as trajectories of particle entering the  $PM_{2.5}$  impactor with a flow rate of 5 L/min. High towards low intensity regions are indicated by red, yellow, green to blue, respectively. Fig. 6(a)

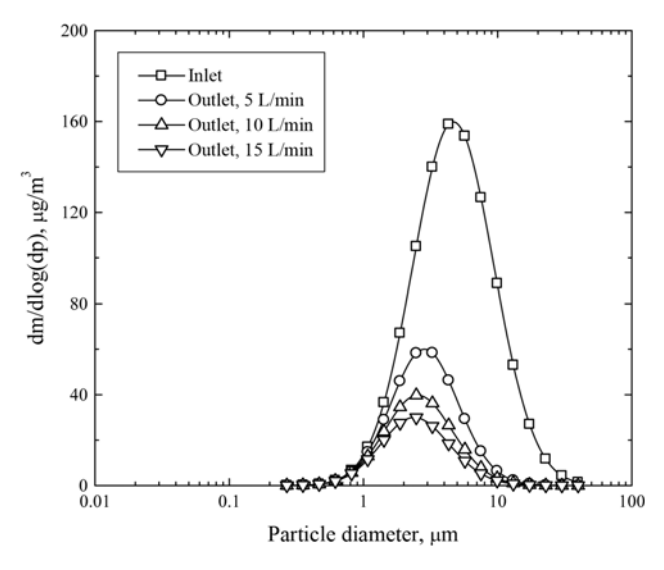


Fig. 5. Theoretical particle size distributions upstream and downstream of the PM<sub>25</sub> impactor.

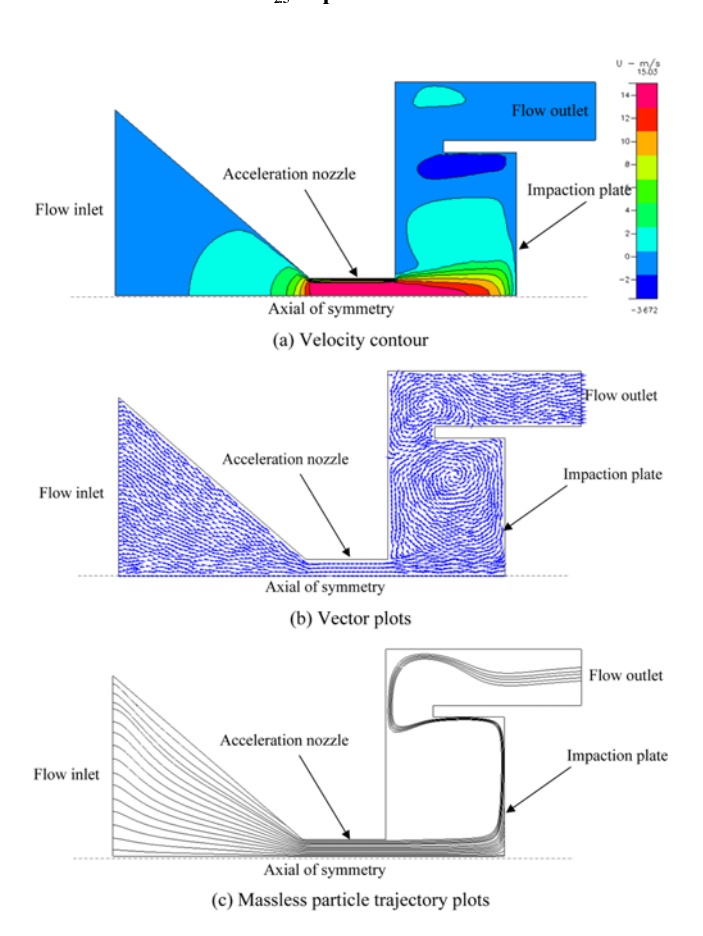


Fig. 6. Numerical results of the velocity contour, vector plots, and particle trajectories in the  $PM_{2.5}$  impactor.

shows the velocity field contours in the  $PM_{25}$  impactor. The highest velocity intensities appeared around the acceleration nozzle and the impaction plate of the impactor. Fig. 6(b) shows the vector plots in the  $PM_{25}$  impactor. A recirculating flow appeared just downstream of the acceleration nozzle outlet of the impactor. Significant partic-

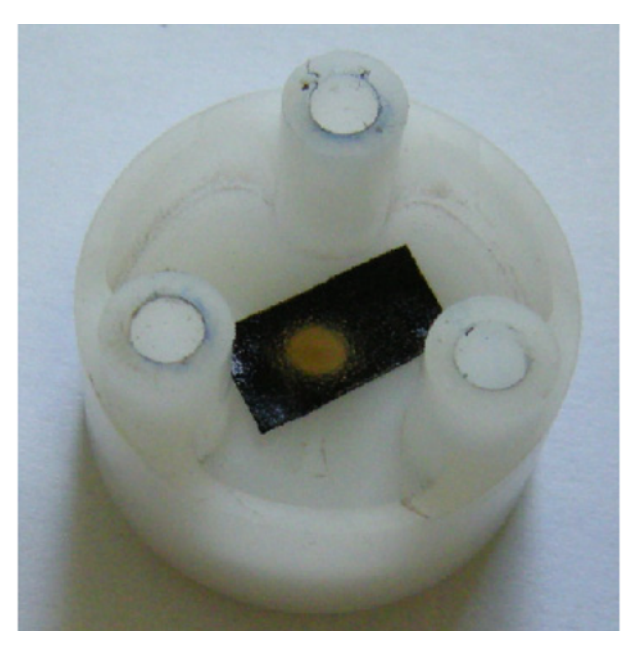


Fig. 7. Typical collected particles on the impaction plate of the  $PM_{25}$  impactor.

ulate loss and particle aggregation due to the inertial force were anticipated here. Trajectory plots of massless particles (i.e., particles whose invariant mass is zero) inside the impactor for both cases are shown in Fig. 6(c). Massless particles were able to follow the streamlines without being collected on the impaction plate.

Fig. 7 shows a photograph of typical particles collected on the impaction plate of the PM25 impactor. Particles agglomerated on the impaction plate. The inherent problems were particle bounce and re-entrainment. These problems in addition to interstage wall losses and non-ideal collection characteristics of the impaction surface have been widely reported [9] for impactor operation. Particle bounce, which can be a severe problem at high velocity, was observed by SEM in the form of agglomerated particles. Fig. 8 shows typical particle morphologies of collected combustion aerosols on the impaction plate of the PM<sub>25</sub> impactor and on the filter. As shown in Fig. 8(a), the collected combustion particles on the impaction plate were widely distributed in size. A large portion of the particles were non-spherical and agglomerated, and the fraction of coagulated particles increased with an increase in collection time of the particles. Their diameter ranged from 2 µm to several micrometers. Fig. 8(b) shows the SEM image of collected combustion particles on the filter. These particles were smaller than 2.5 µm in diameter, agreeing with the theoretical prediction. Similarly, Fig. 9 shows the SEM images of the ambient particles collected on the impaction plate and the filter.

Clearly, the deposited ambient particles on the impaction plate were larger than 2  $\mu m$  in diameter (Fig. 9(a)). The deposited ambient particles on the filter were smaller than approximately 2-3  $\mu m$  in diameter. For comparison, ambient particles were collected by the device projected in this work and the AIRmetrics Minivol portable sampler for 24 hours. From visual inspection, the sampled particulate matter was evenly distributed over the entire active filtration area. The color of the deposit of both filters was very similar. The average particle mass concentrations were found to be in a similar range,

P. Intra et al.

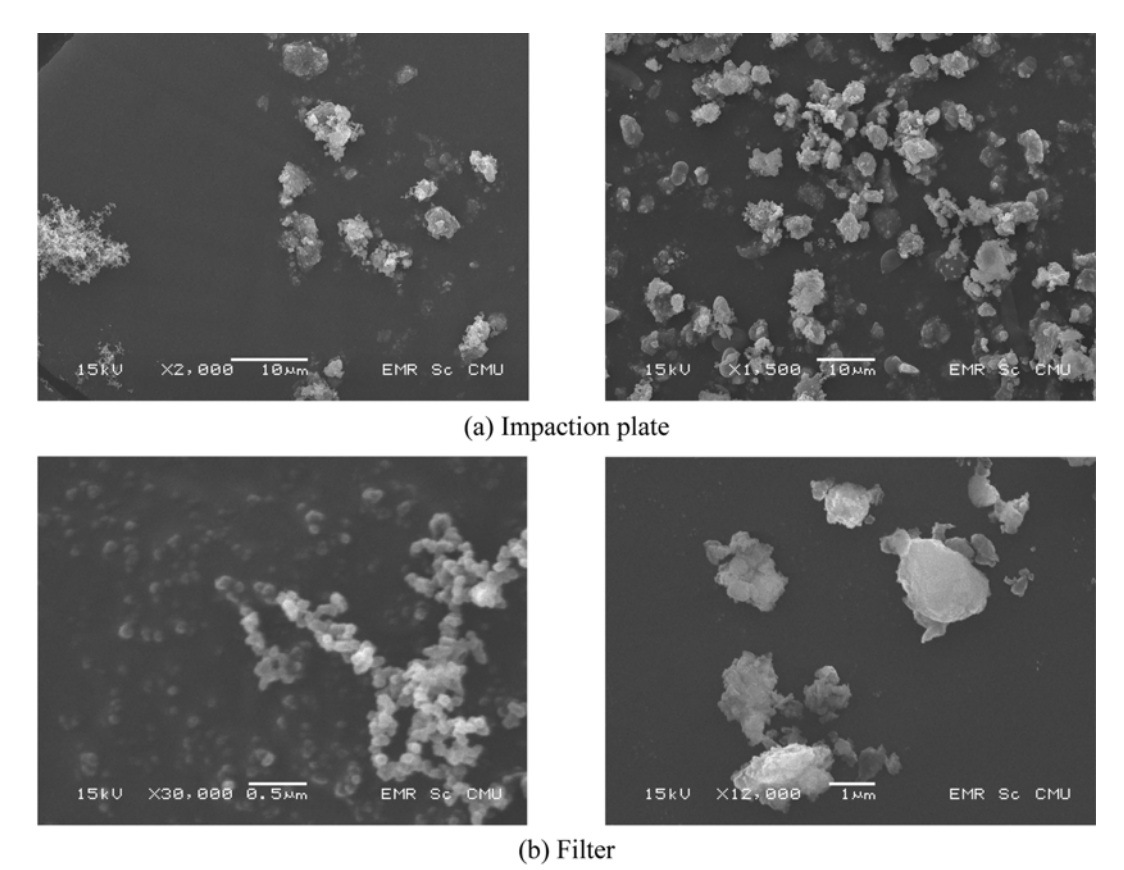


Fig. 8. Typical particle morphologies of collected combustion aerosols.

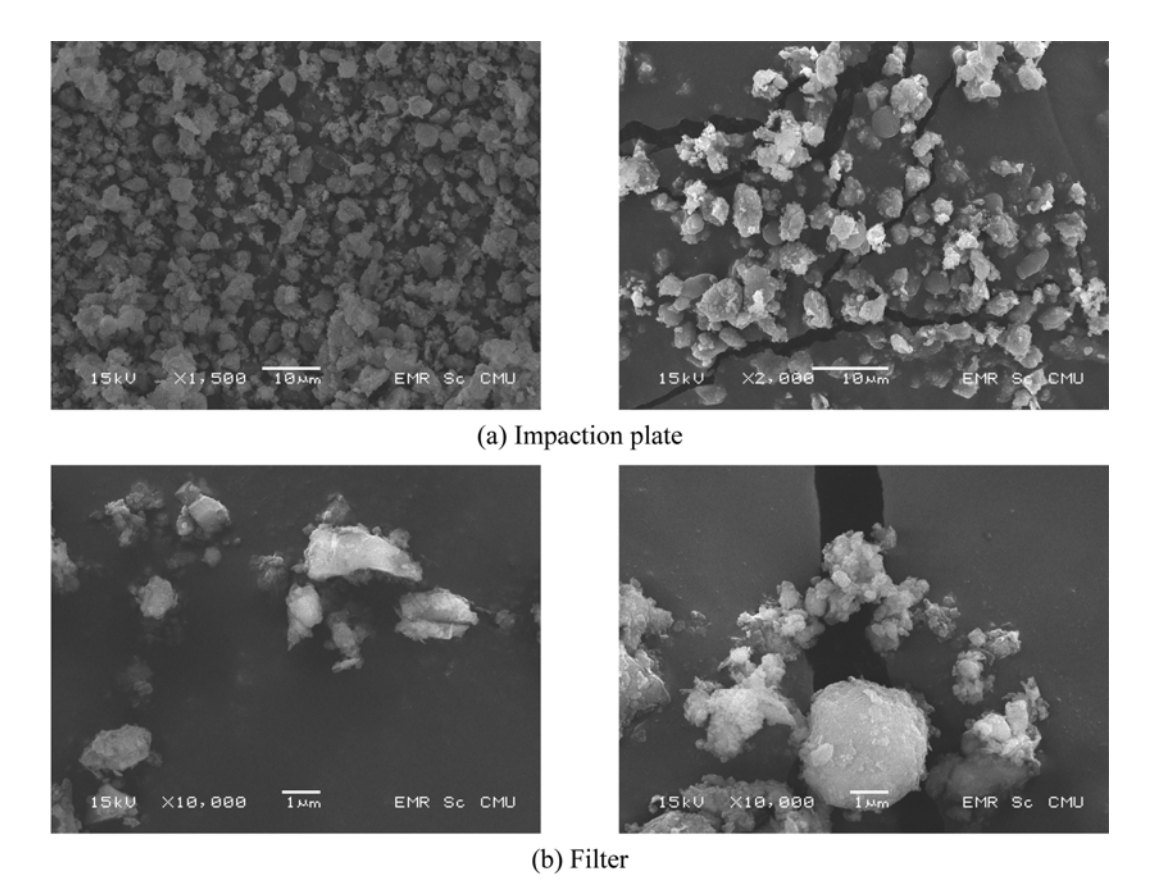


Fig. 9. Typical particle morphologies of collected ambient particles.

between 92 and 95  $\mu$ g/m³ for the present device and the AIRmetrics Minivol portable sampler, respectively. The difference in average mass concentrations from the two samplers was less than 3.5%. The observed difference in the measurements from this work and the AIRmetrics Minivol sampler may be due to different collection areas of the filter and particle losses inside each system. Nonetheless, the collection performance of the present impactor needs be examined further with a system of monodisperse particles from standard sized particles or generated from a setup involving a tandem differential mobility analyzer (DMA). Future verification experiments are planned for this impactor compared to a standard instrument.

## **CONCLUSIONS**

A simple and low cost  $PM_{25}$  sampler for airborne particulate matter has been designed and investigated. The design of the  $PM_{25}$  impactor is based on the inertial impactor configuration of Marple and Willeke [9].

The cut-off diameter of the  $PM_{2.5}$  impactor was analytically investigated by varying the particulate flow rate to predict collection efficiency, flow field and particle trajectory. The cut-off diameter decreased as the flow rate increased.

A numerical model was developed to investigate flow field and particle trajectory inside the impactor to give a better understanding on how the impactor operated. The results of this modeling suggested that an optimal operational domain existed for the  $PM_{2.5}$  impactor. The parameters of the domain were used to build a prototype of the  $PM_{2.5}$  and tested.

The prototype of the PM<sub>2.5</sub> impactor showed promising results for airborne particulate matter sampling. The collected particles on the impaction plate and downstream of the PM<sub>2.5</sub> impactor were analyzed using the SEM. The results agreed well with the theoretical and numerical predictions.

## **ACKNOWLEDGEMENT**

The National Science and Technology Development Agency supported this work: Northern Network, Thailand, contract no. NT-RD-2552-07. We thank Dr. Rainer Zawadzki for editing the manuscript.

#### REFERENCES

- 1. P. Intra and N. Tippayawong, Mj. Int. J. Sci. Tech., 1, 120 (2007).
- W. C. Hinds, *Aerosol technology*, John Wiley & Sons, New York, USA (1999).
- 3. EPA. National Ambient Air Quality Standards for Particulate Matter, Final Rule, Federal Register, **62**, 38651 (1997).

- 4. B. Y. H. Liu and D. Y. H. Pui, Atmos. Environ., 15, 589 (1981).
- A. R. McFarland, C. A. Ortiz and R. W. J. Bertsch, *Environ. Sci. Technol.*, 12, 679 (1978).
- J. B. Wedding, M. A. Weigand and T. C. Carney, *Environ. Sci. Technol.*, 16, 602 (1982).
- 7. P. Intra, CMU. J. Nat. Sci., 7, 257 (2008).
- 8. A. A. Andersen, Am. Ind. Hyg. Assoc. J., 27, 160 (1966).
- 9. V. A. Marple and K. Willeke, *Atmos. Environ.*, **10**, 891 (1976).
- S. V. Hering, R. C. Flagan and S. K. Fliedlander, *Environ. Sci. Technol.*, 12, 667 (1978).
- 11. S. V. Hering, S. K. Fliedlander, J. J. Collins and L. W. Richards, *Environ. Sci. Technol.*, **13**, 184 (1978).
- 12. P. Biswas and R. C. Flagan, J. Aerosol Sci., 19, 113 (1988).
- S. M. Lee, B. D. Chon and S. G Kim, *Korean J. Chem. Eng.*, **8**, 220 (1991).
- H. T. Kim, Y. J. Kim and K. W. Lee, *Aerosol Sci. Technol.*, 29, 350 (1998).
- 15. M. Marjamaki, J. Keskinen, D. R. Chen and D. Y. H. Pui, *J. Aerosol Sci.*, **31**, 249 (2000).
- T. M. Peters, R. W. Vanderpool and R. W. Wiener, *Aerosol Sci. Technol.*, 34, 389 (2001).
- 17. C. H. Huang and C. J. Tsai, Aerosol Air Qual. Res., 2, 01 (2002).
- 18. A. C. Johna, T. A. J. Kuhlbuscha, H. Fissanb, G. Brkerc and K. J. Geuekec, *Aerosol Sci. Technol.*, **37**, 694 (2003).
- 19. D. S. Kim, K. W. Lee and Y. J. Kim, J. Aerosol Sci., 37, 1016 (2006).
- 20. Y. Otani, K. Eryu, M. Furuuchi, N. Tajima and P. Tekasakul, *Aerosol Air Qual. Res.*, **7**, 343 (2007).
- 21. M. Furuuchi, K. Eryu, M. Nagura, M. Hata, T. Kato, N. Tajima, K. Sekiguchi, K. Ehara, T. Seto and Y. Otani, *Aerosol Air Qual. Res.*, **10**, 185 (2010).
- 22. J. J. Cohen and D. N. Montan, *Annals Ind. Hyg. Assoc. J.*, **28**, 95 (1967).
- 23. D. A. Lundgren, J. Air Pollut. Contr. Assoc., 17, 225 (1967).
- 24. V. A. Marple, *Aerosol Sci. Technol.*, **38**, 247 (2004).
- S. Vinchurkar, P. W. Longest and J. Peart, *J. Aerosol Sci.*, 40, 807 (2009).
- W. Winklmayr, H. C. Wang and W. John, Aerosol Sci. Technol., 13, 322 (1990).
- 27. CFD-RC, *CFD-ACE+ User Manual*, http://www.cfdrc.com, Huntsville, USA (2003).
- P. Intra and N. Tippayawong, Int. Conf. on Technology and Innovation for Sustainable Development, Nong Khai, Thailand, 4-6 March (2010).
- 29. W. S. Rasband, *ImageJ*, National Institutes of Health, Bethesda, Maryland, USA (2004).
- K. Willeke and P. A. Baron, *Aerosol Measurement*, John Wiley & Sons, New York, USA (1993).